EVALUATION OF SEISMIC PERFORMANCE OF RC COLUMNS RETROFITTED BY SMA WIRE JACKETS THROUGH FRAGILITY ANALYSIS

E. CHOI[1*], S.H. PARK[1†], J. LEE[1], C. JUNG[1], and Y. EO[1] , Y.S. Chung[2]

[1]*Department of Civil Engineering, Hongik University, Seoul, Korea*
[2]*Department of Civil Engineering, Chung-Ang University, Seoul, Korea*

ABSTRACT

The goal of this study is to provide seismic fragility curves of reinforced concrete columns retrofitted by shape memory alloy wire jackets and thus assess the seismic performance of the columns against earthquakes, comparing them with the reinforced concrete columns with lap-spliced and continuous reinforcement. For that purpose, this study first developed analytical models of the experimental results of the three types of columns, 1) lap-spliced reinforcement, 2) continuous reinforcement and 3) lap-spliced reinforcement and retrofitted by SMA wire jackets, using OpenSEES program, which is oriented to nonlinear dynamic analysis. Then, a suit of ten recorded ground motions was used to conduct dynamic analyses of the analytical models with scaling of peak ground acceleration from 0.1g to 1.0g with increase of 0.1g. From the static experimental tests, the column retrofitted with SMA wire jackets had larger displacement ductility by 2.3 times than the lap-spliced column, which was 6% larger compared with the ductility of the continuous reinforcement column. In the fragility analyses, the SMA wire jacketed column had a median value similar to the continuous reinforcement column for the yield damage state. However, for the complete damage state, the SMA wire jacketed column showed 1.33 times larger median value than the continuously reinforcement column.

Keywords: Fragility analysis, shape memory alloy, seismic retrofit, RC column, nonlinear analysis.

1. INTRODUCTION

Studies on applications of shape memory alloys (SMAs) for civil structures such as steel frames and concrete columns are increasing continuously (Hu et al. 2012; Hu et al. 2011). In a recent decay, SMA wires with shape memory effect (SME) were used to confine the concrete to provide active and passive confining pressure (Andrawes et al. 2010; Choi et al. 2008). Choi and Andrawes

* Corresponding author: Email: eunsoochoi@hongik.ac.kr

† Presenter: Email: phn0603@hanmail.net

performed hysteretic bending tests on the RC columns confined by SMA wires at the base to increase the ductile behavior of the columns (Choi et al. 2012a).

In the RC column tests of Choi et al. (2012a), the SMA wire jackets increased the displacement ductility from that of the as-built column. However, the increment of ductility did not illustrate seismic performance of the column directly under ground motion shakings. Thus, seismic assessment of RC columns requires nonlinear time-history analysis. The goals of this study are to develop fragility curves for the RC columns retrofitted by SMA wire jackets compared them with as-built columns and assess the seismic performance of the SMA wire jacketed column. To archive these goals, this study uses the experimental results of the column conducted in a previous study and develops analytical models corresponding to the experimental data.

2. EXPERIMENTAL TESTS

2.1. Column specimens and retrofit

Lap-splice of reinforcement at the bottom of RC columns produces more problems of low flexural strength and early failure than continuous reinforcement columns (ElGawady et al. 2010; Youm et al. 2007). Thus, such lap-spliced columns need to be retrofitted to increase seismic performance. In this study, three types of specimens are used: 1) a column with lap-spliced reinforcement (which is represented by SP-Non), 2) a column with continuous reinforcement (which is represented by CON-Non), and 3) a lap-spliced column retrofitted by SMA wire jacket (which is represented by SP-SMA). The dimensions and details of the columns are shown in Figure 1.

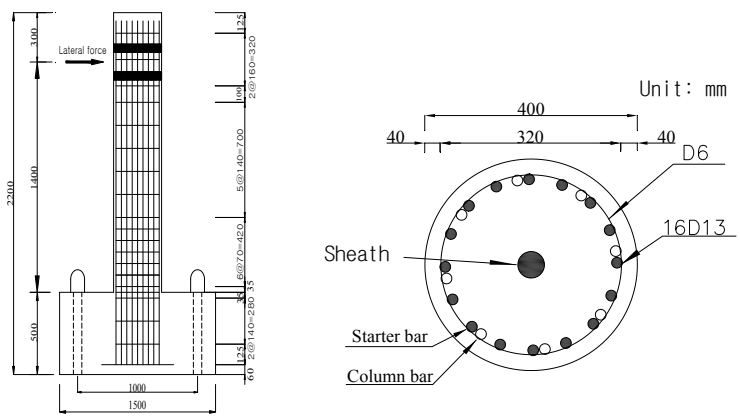

Figure 1: Specimen details.

In the lap-spliced specimen, half of the longitudinal reinforcing bars were spliced from the starter bars projecting from the foundation, which was a 50% lap splice. The peak strength of the concrete and the yield strength of the steel were 24 and 325 MPa, respectively. Additionally, this study prepared Ni47.45-Ti37.86-Nb14.69 (wt.%) SMA wires with a diameter of 1.0 mm. The SMA wires were wrapped around the column at the bottom with a 400 mm length from the base of the

foundation. The remaining residual stress was estimated as 202.8 MPa in the previous study (Choi et al. 2012a).

2.2. Bending tests and results

Quasi-static loading was applied at the top of the columns under displacement control which started from a drift ratio of ±0.25% and then the next step was loading to ±0.5%, which was then increased by 0.5% increments until failure as shown in Figure 2 and each step was applied twice.

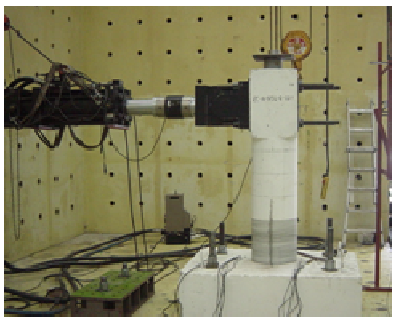

Figure 2: View of test set-up.

The hysteretic lateral force-displacement curves and envelops are shown in Figure 3.

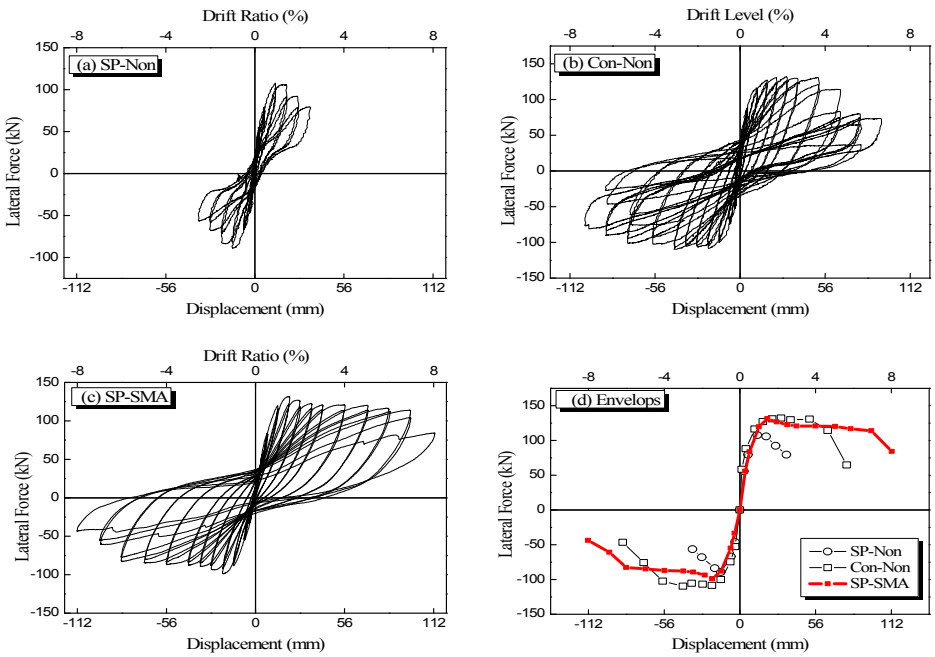

Figure 3: Hysteretic force-displacement curves and their envelopes.

The SMA jacket increased the yield and ultimate force of the specimen SP-SMA specimen by 17% compared to the specimen SP-Non specimen. In the failure drift ratio, the SP-SMA specimen had larger value than both the SP-Non and CON-Non specimens. This was caused from the external pressure on the lap-splice region provided by the SMA wire jacket, which increased the bond strength at the region and delayed the buckling of the longitudinal reinforcing bars at the bottom of

the column. The failure drift ratio of the SP-SMA specimen was much larger than that of the CON-Non specimen. This indicates that the SMA wire jacket was highly effective in delaying the buckling of the longitudinal bars, which was main cause of column failure.

3. ANALYTICAL MODELS OF THE TESTED RC COLUMNS

The analytical platform OpenSEES (2010) was used for this study. The 2-D finite element models of the tested columns were developed. The column was divided into three parts to develop an analytical model: 1) a plastic region with a length of 400 mm from the base, which included a lap-splice region and a SMA jacketing region, 2) a 700 mm length above the plastic region, and 3) a rigid part with a length of 300 mm at the top. The plastic region of the lap-spliced and continuous reinforcing bar had the same kind of section, but the input value that determined the behavior of each model was set differently to reflect the characteristics of each analytical model. In the column retrofitted by a SMA wire jacket, a SMA plate with a thickness of 1 mm with hysteretic behavior was added at the 400 mm length of the column at the bottom to represent the SMA wire jacket. Following the same loading sequence as the experimental tests, calculated hysteretic response of force and displacement were obtained for the three specimens as shown in Figure 4 and Table 1.

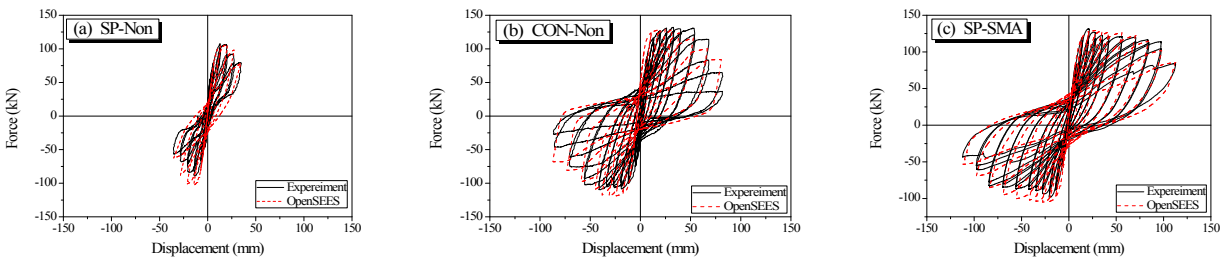

Figure 4: Calculated hysteretic behavior and comparison with experimental responses.

Table 1: Comparison of specific values of analytical models and experimental results

Response	SP-Non		CON-Non		SP-SMA	
	Exp.	Cal.	Exp.	Cal.	Exp.	Cal.
Yield force (kN)	80.8	80.8	99.2	99.2	98.6	98.5
Ultimate force (kN)	107.8	107.7	132.2	132.3	131.5	131.3
Yield drift ratio (%)	0.60	0.64	0.67	0.66	0.95	0.89
Failure drift ratio (%)	1.93	2.20	4.69	4.42	6.67	6.40
Failure ductility factor	3.19	3.43	6.97	6.72	7.40	7.24

4. FRAGILITY ANALYSIS

Analytical fragility curves were obtained from the seismic responses of the analytical models of the structures. The seismic response can be gained from nonlinear time history analysis, elastic response spectrum analysis, or nonlinear pushover analysis.

4.1. Ground motions

A suit of ground motions is required for fragility analysis and this study used ten artificial ground motions simulated on the basis of the recorded ground motions which had the probability of

exceedence of 10% in 50 years for the Los Angeles region of the United States. Moreover, in this study, the ten ground motions were scaled from 0.1g to 1.0g PGA (peak ground acceleration) with increments of 0.1g for the fragility analysis and the response spectra of the ground motions with a PGA of 0.1g are shown in Figure 5.

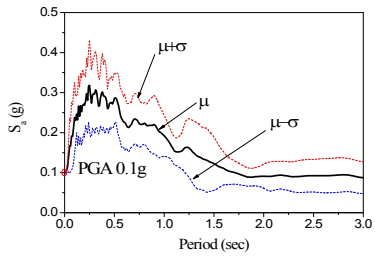

Figure 5: Response spectra and mean of ten artificial ground motions with a PGA of 0.1g.

4.2. Nonlinear time history analysis

The analytical model exhibited perfect elastic behavior before yield as shown in Figure 6(a), and after yielding, stiffness degradation and pinching during unloading were observed as in Figure 6(b). In Figure 6(C), strength degradation was observed around the failure point. In Figure 6(d), however, strength degradation after failure did not occur, which was due to an imperfection of the analytical model.

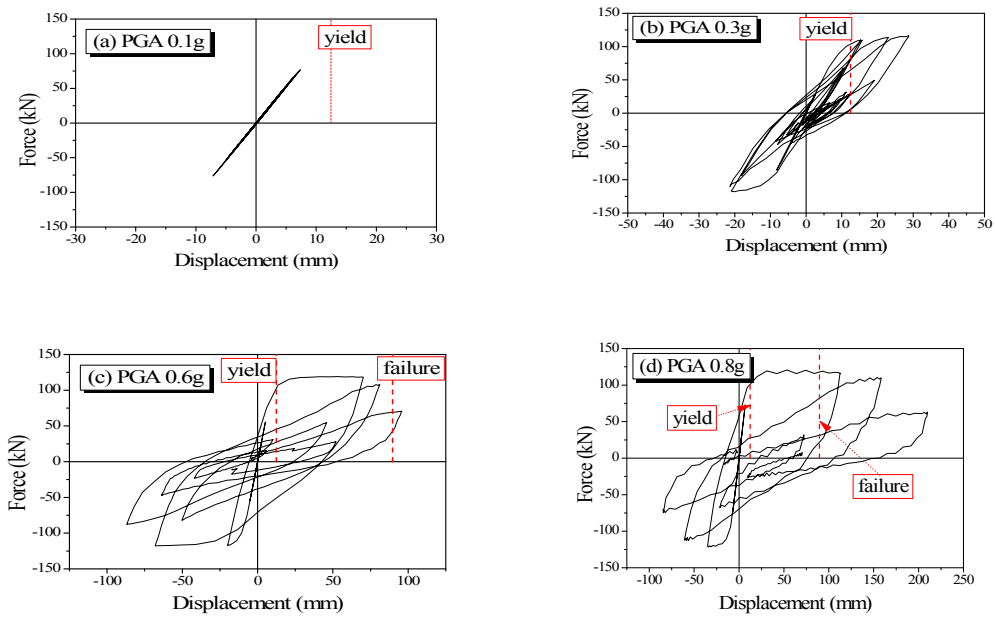

Figure 6: Hysteretic force-displacement curve due to LA02 ground motion for SP-SMA.

4.3. Characterization of damage

In general, most studies on fragility analysis of bridges use five damage states provided by HAZUS-MH (FEMA, 2003). In this study, only the column was estimated and the three behavior states, elastic, yield, and failure, were defined strictly by the method previously mentioned. The elastic behavior state represents no damage and the yield represents slight damage since the yield

point was estimated as a ductility of 1.0, which is the starting range for the slight damage. Failure stands for the complete damage state since it is assumed that the columns lose all function after the failure point. The experimental data of the CON-Non and SP-SMA specimens had ductility of 6.97 and 7.40 at failure. The values are close to the ductility of complete damage in other studies. In the SP-Non specimen, however, the ductility of failure was 3.19, which occurred abruptly after the yield, and thus the moderate or extensive damage states cannot be defined easily.

4.4. Analytical fragility curves

The analytical fragility curves of the columns in this study were developed on the basis of nonlinear time history analyses. A fragility curve describes the probability of reaching or exceeding a damage state as a function of a specific ground motion intensity parameter. The probability of reaching or exceeding a specific damage state with a specific ground motion intensity, which is PGA in this study, will be log-normally distributed, which can be explained by a log-normal cumulative probability density function as follows:

$$P_f\,(Damag \cdot State \cdot i \cdot or \cdot greater / PGA) = \Phi\left[\frac{\ln(x) - \ln(\mu_i)}{\beta_i}\right] \tag{1}$$

where μ and β are the median and dispersion for the *i*th damage state and $\Phi[\bullet]$ is the standard normal distribution function (Shinozuka et al. 2000).

The probabilities were marked with PGA as shown in Figure 7. Using the discrete data of probability, a continuous fragility curve can be obtained by the maximum likelihood method.

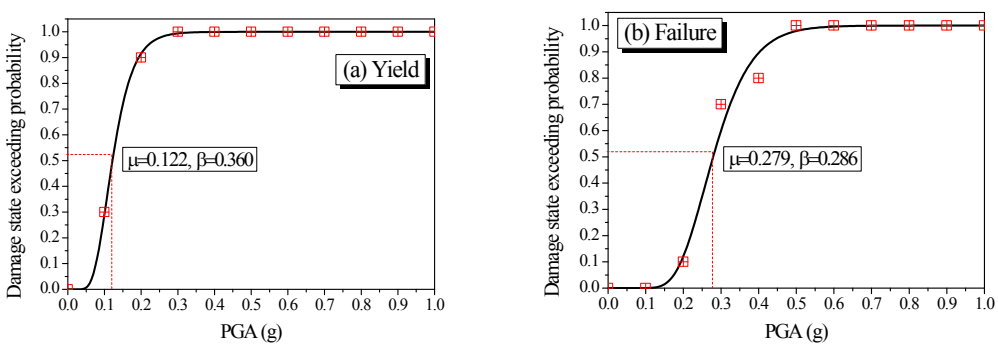

Figure 7: Maximum likelihood method for the SP-Non specimen.

4.5. Results and discussion

Figure 8 show the estimated medians, dispersions and continuous fragility curves for the columns. The CON-Non specimen had the largest median, which was larger by 37.7% than that of the SP-Non specimen and similar to that of the SP-SMA. The yield drift ratio of the SP-SMA specimen was 0.95% which was larger by 58.3% and 41.8% of the other two specimens, respectively. For the failure state, the SP-SMA specimen had the largest median value against the failure and was larger

than those of the other two specimens. In the experimental data, the failure drift ratio of the SP-SMA specimen was 6.67%, which was larger than the other two specimens.

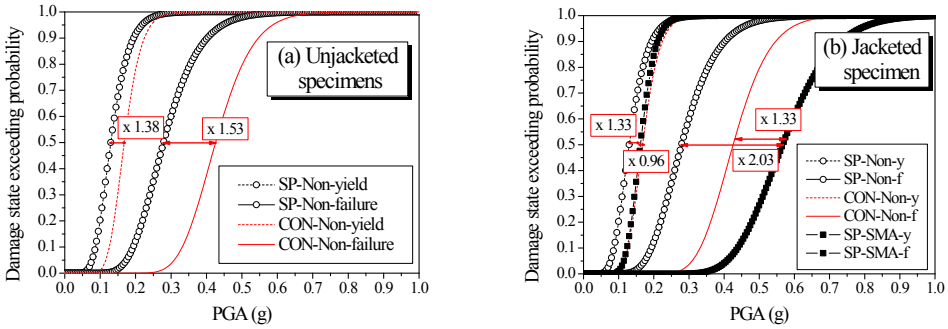

Figure 8: Analytical fragility curves and comparison.

In Korea, which is estimated as a weak or moderate seismic zone, the maximum possible PGA for designing highway or railway bridges is 0.154g. At a PGA of 0.154g, the probability of reaching or exceeding the slight damage state of the SP-Non specimen is 74.3%. Thus, in the Korean peninsula, it is considered that most bridges having such lap-spliced RC columns would be damaged due to yield. In the CON-Non specimen, the probability of reaching or exceeding the slight damage state at the PGA of 0.154g is 35.0%, which is smaller than the half of the probability of the SP-Non specimen. The exceeding probability of the slight damage state was 40.4% for the PGA of 0.154g in the SP-SMA specimen. Therefore, the SMA wire jacket decreased the seismic vulnerability against the yield or slight damage of the lap-spliced column.

When a PGA of 0.154g was applied, the probability of reaching or exceeding the complete damage state for the SP-Non specimen was 18.7%. However, calculating the probability of reaching or exceeding the complete damage state against 0.154g, the values for the CON-Non and SP-SMA specimens were zero. It means that the SMA wire jacket can protect the lap-spliced column from the complete damage state in Korea. Therefore, it is concluded that the SMA wire jacket decreased the vulnerability of the lap-spliced column for slight damage partially and completely removed the possibility of complete damage in weak or moderate seismic zones such as the Korean peninsula.

5. CONCLUDING REMARKS

This study developed analytical models of three types of reinforced concrete columns using the OpenSEES program. The analytical models were well calibrated to trace the experimental hysteretic curves of force-displacement obtained from a previous study. However, in a time history analysis with a ground motion of 0.8g PGA, the curve passed the failure point without unloading after yield and did not show degradation of strength after passing the failure point. The phenomenon did not affect the fragility analysis, but a further study is needed to improve the analytical models based on the static experimental data.

The median values of the three types of columns were obtained from the fragility curves for the damage states. According to the median values of yield and failure, the SMA wire jacket was

effective in reducing the seismic vulnerability of the lap-spliced column. In addition, the median value for failure in the SMA wire jacketed column was larger than that in the column with continuous reinforcement. It was demonstrated that the SMA wire jacket protected the lap-spliced column from the failure, if the column was located in weak or moderate seismic zones such as the Korean peninsula, where the maximum expected PGA is 0.154g. In addition, the probability of exceeding failure in the continuous reinforcing column was 79.5% in the strong seismic region such as the region of California of Mid-America. Thus, it seems that the SMA wire jacket is necessary to reduce seismic vulnerability of failure even for the columns with continuous reinforcement in strong seismic regions.

6. ACKNOWLEDGMENTS

This study was supported by the Basic Science Research Program through the National Research Foundation of Korea funded by the Ministry of Education, Science and Technology (Project No. 2012-0456-03).

REFERENCES

Hu JW, Kim DK, and Choi E (2012). Numerical investigation on the cyclic behavior of smart recentering clip-angle connections with superelastic shape memory alloy fasteners. Journal of Mechanical Engineering Science published online DOI: 10.1177/0954406212459008.

Hu JW, Leon RT, and Choi E (2011). Investigation on the Inelastic Behavior of Full-scale Heavy Clip-angle Connections Inter. Journal of Steel Structures. 11(1). pp. 1-11.

Andrawes B, Shin M, and Wierschem N (2010). Active Confinement of Reinforced Concrete Bridge Columns Using Shape Memory Alloys. Journal of Bridge Engineering, ASCE. 15(1). pp. 81-89.

Choi E, Nam TH, Cho SC, Chung YS, and Park T (2008). The behavior of concrete cylinders confined by shape memory alloy wires. Smart Material and Structure. 17. pp. 065032.

Choi E, Choi DH, Chung YS, and DesRoches R (2012a). Seismic protection of lap-spliced RC columns using SMA wire jackets. Magazine of Concrete Research. 64(3). pp. 239-252

Choi E, Nam TH, Chung YS, Kim YS, and Lee S (2012b). Behavior of NiTiNb SMA wires under recovery stress or prestressing. Nanoscale Research Letters. 7. pp. 66.

ElGawady M, Endeshaw M, McLean D, and Sack R (2010). Retrofitting of Rectangular Columns with Deficient Lap Splices. Journal of Composite for Construction. 14(1). pp. 22-35.

Youm KS, Lee YH, Choi YM, Hwan YK, and Kwon TG (2007). Seismic performance of lap-spliced columns with glass FRP. Magazine of Concrete Research. 59(3). pp.189-198.

OpenSees Development Team (2010). OpenSees: Open system for earthquake engineering simulation. Version 2.21, Berkely, CA, USA.

FEMA (2003) HAZUS-MH. Technical manual Federal Emergency Management Agency. Washington DC.

Shinozuka M, Feng MQ, Lee J and Naganuma T (2000). Statistical Analysis of Fragility Curves. Journal of Engineering Mechanics. ASCE. 126(12). pp. 1224-1231.